Defect Mode Properties and Origin in one Dimensional Photonic Crystal

Vipin Kumar[1]*, B. Suthar[2], J. V. Malik[3], Arun Kumar[4], Kh. S. Singh[5], T.P. Singh[6], A. Bhargva[7]

[1,5]Department of Physics, Digamber Jain College, Baraut-250611, India

[2]Department of Physics, Govt. College of Engineering & Technology, Bikaner 334004, India.

[3,6]Department of Physics, Janta Vedic College, Baraut-250611, India

[4]AITTM, Amity University, NOIDA, India

[7]Nanophysics Laboratory, Department of Physics, Govt. Dungar College, Bikaner 334001 India

[1*]vrpcommon@gmail.com; [2]bhuvneshwer@gmail.com; [3]vk_ccsum@rediffmail.com; [4]arun_mtech@yahoo.co.in; [5]khundrakpam.ss@gmail.com; [6]vrpcommon@indiatimes.com; [7]anamib6@gmail.com;

Abstract

The properties and origin of defect modes in the one dimensional photonic crystal (PC) with a central defect has been studied. Two types of photonic crystals, each having single defect, namely, symmetric and asymmetric PCs are considered. It is found that a defect mode arise at central wavelength for asymmetric PC, whereas two defect modes arise in the vicinity of central wavelength for symmetric PC. These two defect modes can be fixed to a single central defect by increasing the width of the defect layer. But the intensities of these defect modes are found to be different from the intensities of defect modes for asymmetric case. The origin of these defect modes can be explained using impedance matching condition. The propagation characteristics of the proposed structure are analyzed by using the transfer matrix method.

Keywords

Defects; Transfer Matrix Method; Symmetric and Asymmetric PCs; Impedance Matching; Transmittance

Introduction

Photonic crystals (PCs) which are artificial structures with periodically modulated dielectric constants have been attracting a great deal of interest among the researchers particularly for the study of their electromagnetic properties [1-7]. It was observed that periodic modulation of the dielectric functions significantly modifies the spectral properties of the electromagnetic waves. The electromagnetic spectrum in such structures is characterized by the presence of allowed and forbidden photonic energy bands similar to the electronic band structure of periodic potentials. For this reason, such a new class of artificial optical material with periodic dielectric modulation is known as photonic band gap (PBG) material [8]. Fundamental optical properties like band structure, reflectance, group velocity and rate of spontaneous emission, etc. can be controlled effectively by changing the spatial distribution of the dielectric function [4, 5]. Photonic crystal structure has many interesting applications in the field of photonics and optical engineering.

PCs can guide the flow of light inside them, and they have many applications such as localization of the light wave [9], inhibition spontaneous emission [10], lasers [11-13], waveguides [14], splitters [15], antennas [16], optical fibres [17], ultrafast optical switches [18], optical circuits [19], tuneable optical filters [20] and absolute omni-directional PBGs [21-25].

These applications can be realized using pure PCs, but doped or defective PCs may be more useful, just as semiconductor doped by impurities are more important than the pure ones for various applications. The idea of doped PCs comes from the consideration of the analogy between electromagnetism and solid state physics, which lead to the study of band structures of periodic materials and further to the possibility of the occurrence of localized modes in the band gap when a defect is introduced in the lattice. These defect-enhanced structures are called doped photonic crystals and present some resonant transmittance peaks in the band gap corresponding to the occurrence of the localized states [26], due to the change of the interference behaviour of the incident waves. Defect(s) can be introduced into perfect PCs by changing the thickness of the layer [27], inserting another dielectric into the structure [28], or removing a layer from it [29, 30].

PCs with defect(s) have received attention of a huge number of researchers, especially 2D and 3D Pcs, because a great number of applications that can be performed using them. It has been also known that a point defect in 2D PCs can act as a micro-cavity, a line defect in 3D PCs behaves like a waveguide and a planer defect in 3D PCs behaves like a perfect mirror [31, 32]. Similar to 2D or 3D PCs, the introduction of the defect layers in 1D PCs can also create localized defect modes within the PBGs. Due to the simplicity in 1D PCs fabrications as compared to 2D and 3D PCs, the defect mode can be easily introduced in 1D PCs for various applications such as in the design of optical filters and splitters, in the light emitting diodes and in the fabrication of lasers [33-35].

In the present communication, the properties of defect modes for different combinations of materials and the origin of these defect modes have been theoretically studied by using transfer matrix method. The origin of these defect modes can be explained using impedance matching condition.

Theoretical Analysis

The schematic representation of one-dimensional photonic crystal with defect is represented in Figure 1.

We consider two structures (one asymmetric and other symmetric) in which H and L represents the high and low refractive index materials. To compute the transmission spectrum, we employ the transfer matrix method (TMM) [36]. In this method, the transfer matrix for each layer can be written as

$$M_j = F_j P_j F_j^{-1}; \tag{1}$$

where, j stands for H or L layers and F_j and P_j are called the dynamical matrix and the propagation matrix respectively. The dynamical matrix is given by the following equations

$$F_j = \begin{pmatrix} 1 & 1 \\ n_j \cos\theta_j & -n_j \cos\theta_j \end{pmatrix} \text{for TE mode of polarization} \tag{2}$$

and $$F_j = \begin{pmatrix} \cos\theta_j & \cos\theta_j \\ n_j & -n_j \end{pmatrix} \text{for TM mode of polarization} \tag{3}$$

Also, the propagation matrix P_j can be defined as

$$P_j = \begin{pmatrix} e^{i\delta_j} & 0 \\ 0 & e^{-i\delta_j} \end{pmatrix} \tag{4}$$

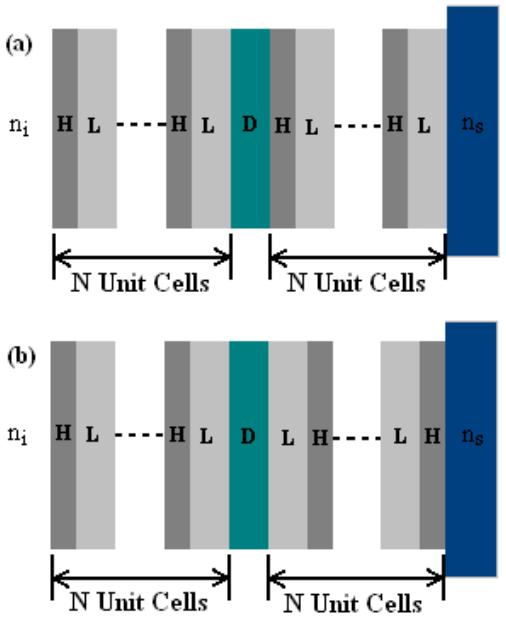

FIG. 1 SCHEMATIC DIAGRAM OF 1-D PHOTONIC CRYSTAL (A) ASYMMETRIC STRUCTURE (B) SYMMETRIC STRUCTURE

where the phase is written as

$$\delta_j = \frac{2\pi d_j}{\lambda} n_j \cos\theta_j \tag{5}$$

The transfer matrix, for the two PCs can be written as

$$M = \begin{pmatrix} M_{11} & M_{12} \\ M_{21} & M_{22} \end{pmatrix} = F_0^{-1} (M_H M_L)^N M_D (M_H M_L)^N F_0 \tag{6}$$

for asymmetric PC

$$M = \begin{pmatrix} M_{11} & M_{12} \\ M_{21} & M_{22} \end{pmatrix} = F_0^{-1} (M_H M_L)^N M_D (M_L M_H)^N F_0$$

for symmetric PC (7)

The reflection and transmission coefficients in terms of the matrix elements, given by Equations (6) and (7), can be written as

$$r = \frac{(M_{11} + q_f M_{12}) q_i - (M_{21} + q_f M_{22})}{(M_{11} + q_f M_{12}) q_i + (M_{21} + q_f M_{22})} \tag{8}$$

and $$t = \frac{2q_i}{(M_{11} + q_f M_{12}) q_i + (M_{21} + q_f M_{22})} \tag{9}$$

where $q_{i,f} = n_{i,f} \cos\theta_{j,f}$ for TE wave and $q_{i,f} = (\cos\theta_{j,f}) / n_{i,f}$ for TM wave, where the subscripts i and f correspond to the quantities respectively in the medium of incidence and the medium of emergence. Whereas, the reflectance and transmittance of the structure is given by

$$R = |r|^2 \text{ and } T = \frac{q_f}{q_i} |t|^2 \tag{10}$$

In the next section, we will compute the transmission spectra of photonic crystal with defect by using

Equation (10) and are represented graphically in Figure 1.

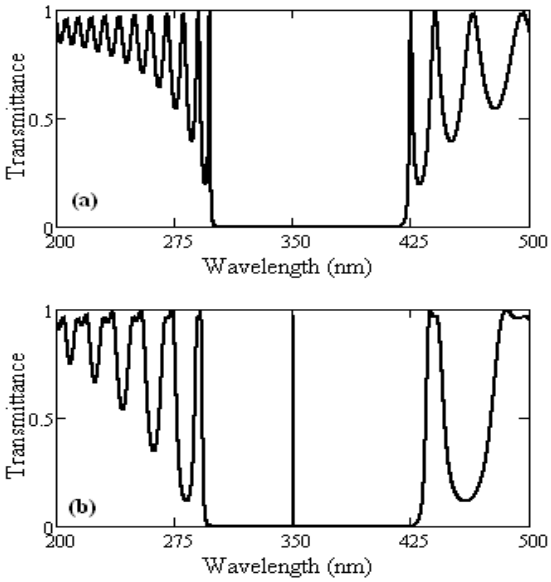

FIG. 2 TRANSMISSION SPECTRA OF (A) AIR/(HL)^{16}/SUBSTRATE (B) AIR/(HL)^{8}D(HL)^{8}/SIO$_2$ STRUCTURE

Results and Discussion

Let us consider a conventional PC- air/(HL)$_{16}$/Substrate that has a Photonic band gap in the ultraviolet and visible regions. In our study, H is taken to be TiO$_2$ with refractive index (n) 2.34867 and L is taken to be MgF$_2$ with n=1.3855. MgF$_2$ is the good material for the PCs because its absorption begins below 115nm and the real part of the refractive index is close to the unity [37]. We use SiO$_2$ (n=1.46) as the substrate. The thickness of each layers is taken according to quarter-wavelength condition i.e. $n_H d_H = n_L d_L = \lambda_0/4$, where λ_0 is the design wavelength and taken to be 350nm. We limit our study to normal incidence only. We have plotted the transmittance properties of this structure using Equation (10). The transmission spectrum of this PC is shown in Figure 2(a). From this figure, it is clear that a PBG is found in the wavelength range of 305-420nm in the vicinity of λ_0. According to the theory of dielectric mirrors, the lower and upper band edges of the band gap can be calculated using the relation given in relation (11) [38, 39].

$$\cos^2\left(\frac{\pi(n_H d_H + n_L d_L)}{\lambda}\right) = k^2 \cos^2\left(\frac{\pi(n_H d_H - n_L d_L)}{\lambda}\right) \quad (11)$$

where $k=(n_H-n_L)/(n_H+n_L)$ is given by the Fresnel formula. By solving Equation (11), we can find the lower and upper edge of the PBG which are λ_L=305nm and λ_H=420nm. If we increase the refractive index contrast (n_H/n_L), the width of the PBG increases accordingly. If we introduce a defect SiO$_2$ (n=1.46) layer in the middle of this conventional PC, then a defect mode is found at the designing wavelength λ_0 in the PBG as shown in Figure 2(b). Our aim is to study this defect mode for various materials namely SiO$_2$, Al$_2$O$_3$, Bi$_4$Ge$_3$O$_{12}$ (BGO), ZnS. We consider asymmetric and symmetric PC structures for our study. Also, the origin of these defect modes explained using impedance matching condition.

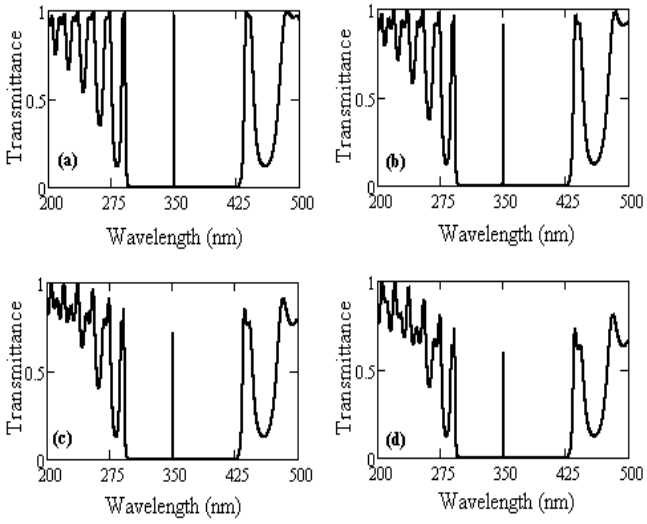

FIG. 3 TRANSMISSION SPECTRA OF AIR/(HL)^{8}D(HL)^{8}/SIO$_2$ STRUCTURE ($D_D = \Lambda_0/4N_D$) FOR (A) D=SIO$_2$ (B) D=AL$_2$O$_3$ (C) D=BGO (D) D=ZNS

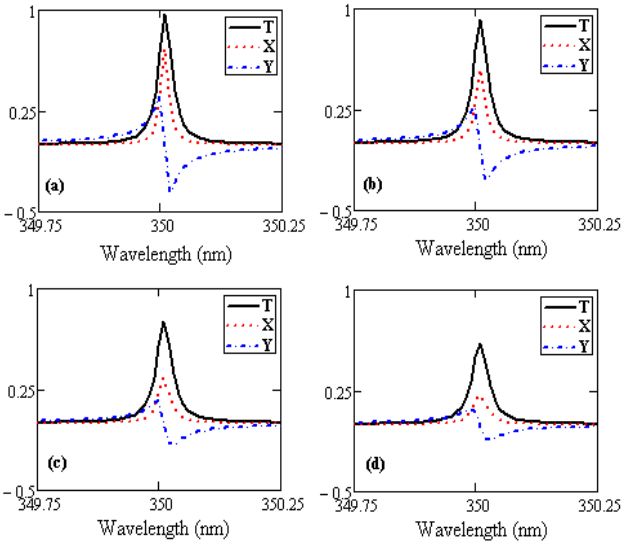

FIG. 4 PLOT OF T (EQUATION (10)), X AND Y (EQUATION (12)) IN THE VICINITY OF THE DEFECT MODES OF FIGURE 3

Effect of the Defect Material on Defect Mode

(1) Asymmetric PC structure air/(HL)$_8$/D/(HL)$_8$/SiO$_2$

For this case we choose the materials whose refractive indices are same as that of H and L layers considered for the conventional PC. For the defect layer D, we

choose four different materials SiO_2 (n=1.46), Al_2O_3 (n=1.66574), BGO (n=2.13) and ZnS(n=2.58789) [40]. The thickness of the defect layer is also chosen so that quarter wavelength condition i.e. $d_D = \lambda_0/4n_D$ is satisfied by the defect layer. The transmission spectra for these structures, each with a defect, are shown in Figure 3(a-d). From these figures, it is clear that for all structures with defect of different materials, the defect modes are found at the same wavelength λ_0. But the intensities of these defect modes (transmitted) are different for different materials. The intensity is maximum for the material whose refractive index is closer to the refractive index of low refractive index material i.e. MgF_2. If we increase the refractive index of the defect layer, then the intensity of defect modes decreases.

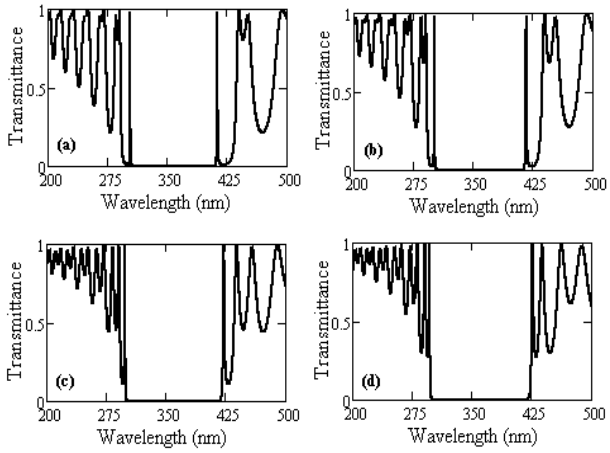

FIG. 5 TRANSMISSION SPECTRA OF AIR/(HL)^{8}D(LH)^8/SIO_2 STRUCTURE ($D_D = \Lambda_0/4N_D$) FOR (A) D=SIO_2 (B) D=AL_2O_3 (C) D=BGO (D) D=ZNS

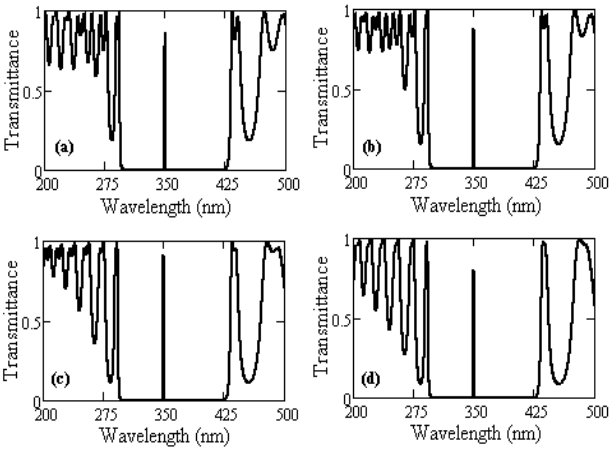

FIG. 6 TRANSMISSION SPECTRA OF AIR/(HL)^{8}D(HL)^8/SIO_2 STRUCTURE ($D_D = \Lambda_0/2N_D$) FOR (A) D=SIO_2 (B) D=AL_2O_3 (C) D=BGO (D) D=ZNS

The origin of these defect modes can be explained using impedance matching condition [38]. The normalized effective surface impedance, z at the incident plane boundary is given by

$$z = X + iY = \frac{Z}{Z_0} = \frac{1+r}{1-r} \tag{12}$$

where Z_0=377Ω, is the intrinsic impedance of the free space, Z is the effective surface impedance at the incident plane boundary and r is the reflection coefficient defined by Equation (8). The real part X, imaginary part Y (Equation (12)) and transmittance, T are plotted in Figure 3(a-d) in the vicinity of defect modes. From these Figures, it is seen that the defect mode is observed only when the condition of impedance matching is satisfied. In these Figures, we have found an anomalous behaviour in real part X of the effective surface impedance Z. The intensity of defect modes is found be maximum corresponding to the strong dispersion of X and it is, however, be minimum corresponding to weak dispersion of X.

(2) Symmetric PC structure air/$(HL)^8$/D/$(LH)^8$/SiO_2

For this case, we choose the same materials as taken in case (1). The transmission spectra for symmetric structure for different materials are shown in Figures 5(a-d). From these Figures, it is clear that in this case, two defect modes are found near the band edges of the PBG. These defect modes disappear if we increase the refractive index of the defect layer (Figure 5(d)).

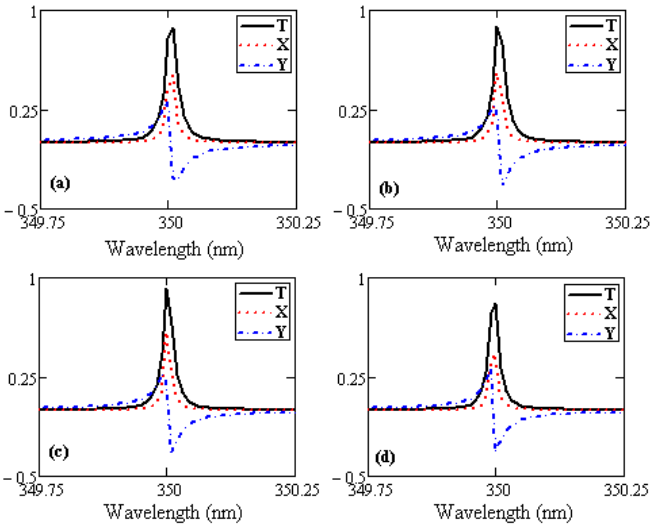

FIG. 7 PLOT OF T (EQUATION (10)), X AND Y (EQUATION (12)) IN THE VICINITY OF THE DEFECT MODES OF FIGURE 6

On the other hand these defect modes can be fixed to a single defect mode at the design wavelength (λ_0) by increasing the width of the defect layer twice its previous value i.e. $d_D = \lambda_0/2n_D$. The transmission spectra for this case are shown in Figure 6(a-d). From

these Figures it is clear that the intensity of each of these defect modes is more for those defect materials whose refractive index is close to the high refractive index material (H). For this case the plot of X, Y and T is shown in Figure 7(a-d). From these Figures it is clear that there is a strong dispersion corresponding to a high intensity of the defect mode.

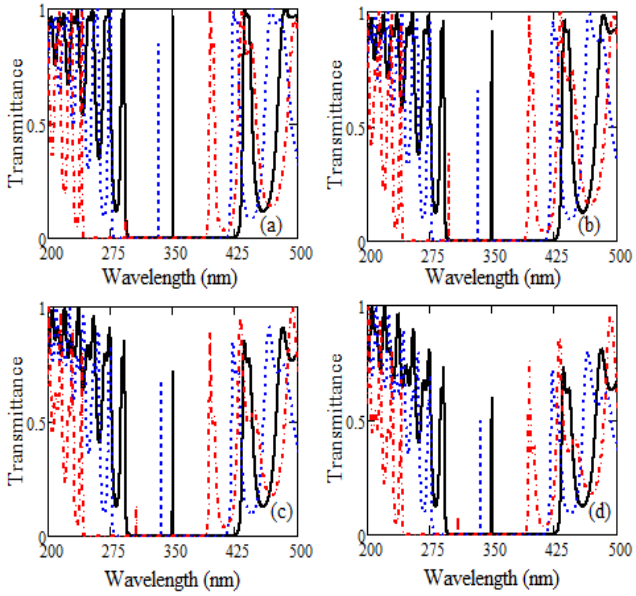

FIG. 8 TRANSMISSION SPECTRA OF AIR/(HL)^{8}D(HL)^8/SIO$_2$ STRUCTURE ($D_D = \Lambda_0/4N_D$) FOR (A) D=SIO$_2$ (B) D=AL$_2$O$_3$ (C) D=BGO (D) D=ZNS AT DIFFERENT ANGLES OF INCIDENCE 0º (BLACK SOLID LINE), 30º(BLUE DOTTED LINE) AND 60º (RED DASHED LINE)

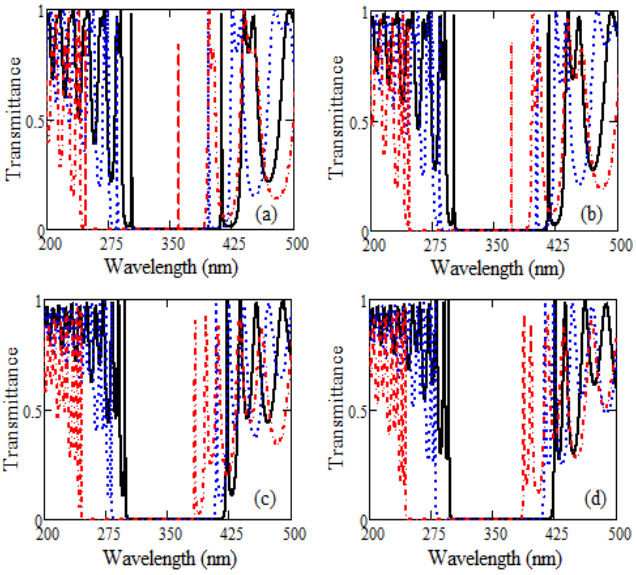

FIG. 9: TRANSMISSION SPECTRA OF AIR/(HL)^{8}D(LH)^8/SIO$_2$ STRUCTURE ($D_D = \Lambda_0/4N_D$) FOR (A) D=SIO$_2$ (B) D=AL$_2$O$_3$ (C) D=BGO (D) D=ZNS AT DIFFERENT ANGLES OF INCIDENCE 0º (BLACK SOLID LINE), 30º(BLUE DOTTED LINE) AND 60º (RED DASHED LINE)

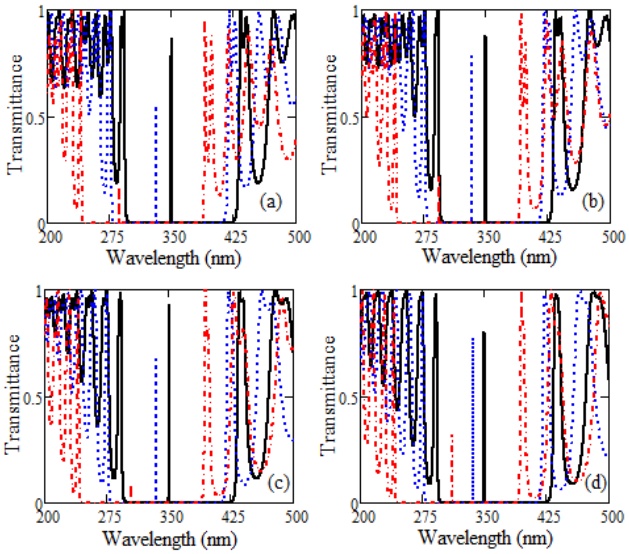

FIG. 10: TRANSMISSION SPECTRA OF AIR/(HL)^{8}D(LH)^8/SIO$_2$ STRUCTURE ($D_D = \Lambda_0/2N_D$) FOR (A) D=SIO$_2$ (B) D=AL$_2$O$_3$ (C) D=BGO (D) D=ZNS AT DIFFERENT ANGLES OF INCIDENCE 0º (BLACK SOLID LINE), 30º(BLUE DOTTED LINE) AND 60º (RED DASHED LINE)

Effect of Angle of Incidence on Defect Mode

(1) Asymmetric PC structure air/(HL)^8/D/(HL)^8/SiO$_2$

In case of the asymmetric structure, the transmission spectra for different defect layers SiO$_2$, Al$_2$O$_3$, BGO and ZnS with defect thickness $d_D = \lambda_0/4n_D$, at different angles (0º, 30º and 60º) of incidence are shown in Figures 8. From this Figure, it is clear that the defect modes shift towards the lower edge of the band gap as we increase the angle of incidence. Also the intensity of these defect modes decreases with increase the angle of incidence. It is also clear that the intensity of these defect modes decreases with fewer amounts for those defect materials whose refractive index is close to the $(n_H - n_L)/2$.

(2) Symmetric PC structure air/(HL)^8/D/(HL)^8/SiO$_2$

In case of the symmetric structure, the transmission spectra for different defect layers SiO$_2$, Al$_2$O$_3$, BGO and ZnS with defect thickness $d_D = \lambda_0/4n_D$, at different angles (0º, 30º and 60º) of incidence are shown in Figure 9. From these Figures, it is clear that in this case, two defect modes are found near the band edges of the PBG at normal incidence. As we increase the angle of incidence the left defect mode disappear whereas the right defect mode shifts towards the left. Both defect modes disappear with the increment of the refractive index of the defect mode. Also the intensity of these defect modes decreases with increase the angle of incidence. These defect modes disappear if we increase the refractive index of the defect layer.

On the other hand these defect modes can be fixed to a single defect mode at the design wavelength (λ_0) by increasing the width of the defect layer twice its previous value i.e. $d_D = \lambda_0/2n_D$. For this case of the symmetric structure, the transmission spectra for different defect layers SiO_2, Al_2O_3, BGO and ZnS at different angles of incidence (0º, 30º and 60º) are shown in Figures 10. From this Figure, it is clear that the defect modes shift towards the lower edge of the band gap as we increase the angle of incidence. Also the intensity of these defect modes decreases with increase the angle of incidence. In this case, the intensity of the defect modes decreases in the different way from the asymmetric case.

Conclusions

Based on the Transfer Matrix Method, the properties and origin of defect modes in one dimensional photonic crystal have been theoretically studied. It is found that we can achieve the desired intensities of defect modes using symmetric and asymmetric structures and the thickness of the defect layer according to our requirement. These defective PCs can be used as single and multi channel filters. Specially, the symmetric defective PC can be used also in DWDM applications.

REFERENCES

E. Yablonvitch, "Inhibited spontaneous emission in solid-state physics and electronics", *Phy. Rev. Lett.*, vol. 58, no. 20, pp. 2059-2062, 1987.

K. M. Ho, C. T. Chan and C. M. Soukoulis, "Existence of a photonic gap in periodic dielectric structures**",** *Phys. Rev. Lett.*, Vol. 65, pp. 3152, 1990.

J. D. Jonopoulos, P. Villeneuve and S. Fan, "Photonic crystals: putting a new twist on Light", *Nature*, Vol. 386, pp. 143, 1997.

J. A. M. Rojas, J. Alpuente, J. Pineiro, and R. Sanchez, "Rigorousfull vectorial analysis of electromagnetic wave propagation in 1D", *Prog. Electromagn. Res.*, Vol. 63, pp. 89-105, 2006.

E. Yablonovitch and T. J. Gmitter, "Photonic band structure: The face-centered-cubic case", *Phys. Rev. Lett.*, Vol. 63, pp. 1950, 1989.

J. D. Joannopoulos, R. D. Meade and J. N. Winn, Photonic Crystals: Molding the Flow of Light, Princeton Univ. Press, Princeton, NJ, 1995.

E. Burstein and C. Weisbuch, Confined Electron and Photon:New Physics and Applications, Plenum Press, New York, 1995.

C. Soukoulis, Photonic Band Gap Materials, 71–79, Kluwer Academic, Dordrecht, 1996.

S. John, "Strong localization of photons in certain disordered dielectric superlattices", *Phys. Rev. Lett.*, Vol. 58, pp. 2486-2489, 1987.

M. Boroditsky, R. Vrijen, T. F. Krauss, R. Coccioli, R. Bhat and E. Yablonovitch, "Spontaneous emission extraction and Purcell enhancement from thin-film 2-D photonic crystals", *J. Lightwave Technol.*, Vol. 17, pp. 2096-2112, 1999.

O. Painter, R. K. Lee, A. Scherer, A. Yariv, J. D. O'Brien, P. D. Dapkus and I. Kim, "Two dimensional photonic band gap defect mode laser", *Science*, Vol. 284, pp. 1819-1821, 1999.

A. Mekis, M. Meier, A. Dodabalapur, R. E. Slusher and J. D. Joannopoulos, "Lasing mechanism in two-dimensional photonic crystals lasers", *Appl. Phys. A: Materials Science and Processing*, Vol. 69, pp. 111-114, 1999.

S. Noda, M. Yokoyama, M. Imada, A. Chutinan and M. Mochizuki, "Polarization mode control of two-dimensional photonic crystal laser by unit cell structure design", *Science*, Vol. 293, pp. 1123-1125, 2001.

A. Mekis, J. C. Chen, I. Kurland, S. Fan, P. R. Villeneuve and J. D. Joannopoulos, "High transmission through sharp bends in photonic crystals waveguides", *Phys. Rev. Lett.*, Vol. 77, pp. 3787-3790, 1996.

T. Sondergaard and K. H. Dridi, "energy flow in photonic crystal waveguides", *Phys. Rev. B*, Vol. 61, pp. 15688-15696, 2000.

E. R. Brown, C. D. Parker and E. Yablonovitch, "Radiation properties of a planner antenna on a photonic crystal substrate", *J. Opt. Soc. Am. B*, Vol. 10, pp. 407-410, 1993.

J. C. Knight, J. Broeng, T. A. Birks and P. St. J. Russell, "Photonic band gap guidance in optical fibers", *Science*, Vol. 282, pp. 1476-1479, 1998.

P. R. Villeneuve, D. S. Abrams, S. Fan and J. D. Joannopoulos, "Single-mode waveguide microcavity for fast optical switching", *Opt. Lett.*, Vol. 21, pp. 2017-2019, 1996.

H. Kosaka, T. Kawashima, A. Tomita, M. Notomi, T. Tamamura, T. Sato and S. Kawakamib, "Photonic crystals for micro lightwave circuits using wavelength

dependent angular beam steering", *Appl. Phys. Lett.*, Vol. 74, pp. 1370-1372, 1999.

S. K. Awasthi and S. P. Ojha, "Design of a tunable optical filter by using a one-dimensional ternary photonic band gap material", *Prog. Electromagn. Res. M*, Vol. 4, pp. 117-132, 2008.

Dowling, J. P., "Mirror on the wall: You're omnidirectional after all?", *Science*, Vol. 282, 1841, 1998.

E. Yablonovitch, "Engineered omnidirectional external-reflectivity spectra from one-dimensional layered interference filters", *Opt. Lett.*, Vol. 23, pp. 1648, 1998.

D. N. Chigrin, A. V. Lavrinenko, D. A. Yarotsky and S. V. Gaponenko, "Observation of total omnidirectional reflection from a one dimensional dielectric lattice", *Appl. Phys. A: Mater. Sci. Process.*, Vol. 68, pp. 25, 1999.

B. Suthar, V. Kumar, Kh.S. Singh and A. Bhargava, "Tuning of photonic band gaps in one dimensional chalcogenide based photonic crystal", *Opt. Commun.*, Vol. 285, pp. 1505, 2012.

V. Kumar, Kh. S. Singh, S. K. Singh and S. P. Ojha, "Broadening of omnidirectional photonic band gap in si-based one dimensional photonic crystals", *Prog. Electromagn. Res. M*, Vol. 14, pp. 101-111, 2010.

G. Guida, A. de Lustrac and P. Priou, "An Introduction to Photonic Band Gap (PBG) Materials", *Prog. Electromagn. Res.*, Vol. 41, pp. 1-20, 2003.

B. Suthar and A. Bhargava, "Temperature-Dependent Tunable Photonic Channel Filter", *IEEE: Photon. Tech. Lett.*, Vol. 24, no. 5, pp. 338-340, 2012.

C. M. Soukoulis, Photonic band gaps and localization, NATO ARW, Plenum Press, New York, 1993.

D. R. Smith, R. Dalichaouch, N. Kroll and S. Schultz, "Photonic band structure and defects in one and two dimensions", *J. Opt. Soc. Am. B*, Vol. 10, no. 2, pp. 314-321, 1993.

V. Kumar, Kh. S. Singh and S. P. Ojha, "Abnormal behaviour of one-dimensional photonic crystal with defect", *Optik* 122, pp. 1183–1187, 2011.

J. D. Joannopoulos, R. D. Meade and J. N. Winn, Photonic Crystal: Molding Flow of Light, Princeton Univ. Press, Princeton, 1995.

H. Y. Lee and T. Yao, "Design and evaluation of omnidirectional one dimensional photonic crystals", *J. Appl. Phys.*, Vol. 93, pp. 819-830, 2003.

Z. M. Jiang, B. Shi, D.T. Zhao, J. Liu and X. Wang, "Silicon-based photonic crystal heterostructure", *Appl. Phys. Lett.*, Vol. 79, pp. 3395-3397, 2001.

M. W. Feise, I. V. Shadrivov and Y. S. Kivshar, "Bistable diode action in left-handed periodic structures", *Phys. Rev. E* 71, pp. 037602, 2005.

W. D. Zhou, J. Sabarinathan, P. Bhattacharya, B. Kochman, E. W. Berg, P. C. Yu and S. W. Pang, "Characteristics of a photonic bandgap single defect microcavity electroluminescent device", *IEEE: J. Quantum Electron*, Vol. 37, pp. 1153-1160, 2001.

P. Yeh, Optical Waves in Layered Media, John Wiley and Sons, New York,1988.

Y. Wu, M. Gu, E. Cao, R. Xum and L. Chen, "Design of a one-dimensional photonic crystal for the modification of BaF_2 scintillation spectrum", *Nuclear Instrum. Methods Phys. Res. A*, Vol. 496, pp. 129, 2003.

Hui-Chuan Hung, Chien-Jang Wu and Shoou-Jinn Chang, "Terahertz temperature-dependent defect mode in a semiconductor-dielectric photonic crystal", *J. Appl. Phys.*, Vol. 110, pp. 093110, 2011.

S. J. Orfanidis, Electromagnetic Waves and Antennas (Rutger University, NJ, 2008), Chapter 7.

Ghosh, G.: Handbook of thermo-optic coefficients of optical materials with applications, Academic Press, New York (1985).

Vipin Kumar was born on July 10, 1980, in Sirsali, Uttar Pradesh, India. He received the B.Sc. degree in 1999, M.Sc. degree in Physics in 2001 and Ph.D. degree in Photonics in 2012 from the C.C.S. University, Meerut, U.P., India.

He qualified national-level examinations, namely, Graduate Aptitude Test in Engineering, National Eligibility Test and Joint Entrance Screening Test. He has fifteen published papers in national and international level journals. His research interests include Optoelectronics, Photonics, and Nonlinear Optics.